IEEJ Journal of Industry Applications
Vol.6 No.5 pp.320–327 DOI: 10.1541/ieejjia.6.320

Paper

Resonance-suppression Control for Electro-hydrostatic Actuator as Two-inertia System

Kenta Tsuda* Non-member, Tomoki Sakuma* Non-member
Kodai Umeda* Non-member, Sho Sakaino* Senior Member
Toshiaki Tsuji* Senior Member

(Manuscript received Feb. 8, 2017, revised May 16, 2017)

Electro-hydrostatic actuators (EHAs) are hydraulic actuators with high power-to-weight ratios that exhibit low energy loss. Thus far, methods for determining the characteristics and parameters of EHAs have not been fully established. Therefore, modeling methods for EHA are in demand. EHAs are driven by servomotors on the motor-side and hydraulic motors on the load-side, and therefore, the actuators are expected to experience sympathetic vibrations. Thus, EHAs can be considered as systems in which two rigid objects are connected to one another with a low-rigidity shaft such as a spring. The occurrence of resonance in EHAs has not yet been discussed because of difficulties with hydraulic systems. One major problem is the large friction in hydraulic motors. We apply a feedback modulator for friction compensation to enable the experimental identification of characteristics. Assuming that EHAs experience two-inertia resonance, the parameters of the motors can be calculated. In addition, vibration-suppression techniques for two-inertia systems can be applied to EHAs. This study proposes the application of a two-inertia model to suppress vibrations in EHAs and verify their dynamic characteristics.

Keywords: electro-hydrostatic actuator, hydraulic closed-loop circuit, two-inertia system, resonance ratio control

1. Introduction

In recent years, the demand for actuators with high power-to-weight ratios has increased in the field of mechatronics. This trend not only extends to the field of construction and heavy equipment, in which robots with large output are in demand, but also to environmental fields of human assistance such as nursing care [1]–[3].

Hydraulic actuators generally have higher power-to-weight ratios than other types of actuators, such as electric ones. These ratios result from the separation of the driving units and actuators. Hydraulic actuators also allow considerable freedom in the system design [4]. The driving units of hydraulic actuators include electric motors, oil tanks, servo units, and hydraulic pumps in addition to power sources. The hydraulic actuators are controlled by regulating the amount of oil discharged into the motor pumps through pipes. The servo units are formed of two types of hydraulic circuits: open- and closed-loop circuits. Open-loop circuits have servo valves that control the flow of oil. Since servo valves separate servo units and actuators, an external force cannot be delivered to the servo units. This makes open-loop hydraulic circuits non-backdrivable systems [5]. Hydraulic actuators with open-loop circuits have been employed primarily in the construction industry as multiple servo valves can connect to actuators via motor pumps.

Hydraulic closed-loop circuits have smaller and more efficient systems than open-loop circuits as driving units are closed within servo units and actuators [4]. Electro-hydrostatic actuators (EHAs), which are hydraulic actuators comprising closed-loop circuits with displacement volume-controlled systems, have been developed [6][7]. In addition, several studies on the dynamics of EHAs and methods to identify parameters have aimed to improve control and cost performances [8]–[11]. However, since EHAs suffer from numerous nonlinearities such as friction and oil leakage inside the hydraulic motor [12]–[14], there have been few modeling studies. Therefore, further studies of the characteristics of EHAs are necessary, along with the development of modeling methods.

EHAs contain servomotors that run the hydraulic pumps connected to one another as drives and discharge oil through the valves to the load-sides, which are hydraulic motors. Thus, if the pressurized oil in the valves has the characteristics of a spring because of its compressibility, EHAs can be considered as systems in which two rigid objects are connected to one another with a low-rigidity shaft. The twisting resonances of the shaft are expected to cause on the actuators in EHAs as well as in general industrial machines [15]–[17]. If resonance occurs, EHAs can be described as two-inertia systems; i.e., an EHA would have two inertias with a low-rigidity shaft, resulting in resonance from the torsional twisting between them. A servo-pump-control approach in which EHAs are modeled as two-inertia systems has been proposed [18]. However, the occurrence of resonance in EHAs has not yet been discussed because of friction in the hydraulic motors, which has caused major difficulties for identifying the dynamic characteristics of EHAs.

* Graduate School of Science and Engineering, Saitama University
255, Shimo-ohkubo, Sakura-ku, Saitama 338-8570, Japan

Hydraulic actuators exhibit dead zones in the low-speed domain because of massive friction compared to electric and pneumatic actuators [19]–[21]. The static friction in EHAs has to be compensated in order to measure the characteristics. Consequently, friction-compensating methods including the application of dithered signals and pulse-width modulation control have been studied [22]. However, these methods are not suitable for EHAs, as they rely on the response performance of the servo valves. Therefore, a feedback modulator (FM) has been considered suitable for practical implementation of EHAs [23]. In FMs, controllers that include integrators (e.g., disturbance observers [24]) generate residual oscillation when friction is large. The dynamic characteristics of EHAs can be measured by the application of FMs.

If EHAs can be modeled as two-inertia systems, vibration-suppression-control methods can be utilized. Several studies have been performed on vibration suppression in two-inertia systems [25]–[28].Generally, information about the motor-side and load-side positions is required to control two-inertia systems [15]. Various studies have also been performed on control methods for two-inertia systems; e.g., a method that utilizes only the load-side information with a high-resolution encoder has been proposed [29], and a resonance-ratio technique has been applied to suppress vibrations caused by the two-inertia resonance [30].

This study proposes to model EHAs as two-inertia systems and identify their dynamic characteristics based on their frequency characteristics. By applying FMs, resonance characteristics can be investigated. To the best of the authors' knowledge, this is the first study to investigate the resonance characteristics of EHAs. The inertia moments of EHAs are obtained by resonance characteristics; these parameters are necessary for applying resonance-suppression control to EHAs. Finally, the control performance is improved by the resonance-ratio technique.

This paper comprises seven sections. Sections 2 and 3 describe a hydraulic circuit of EHAs and a two-inertia model, respectively. An experimental setup is discussed in Section 4, and the controllers used in the experiment are explained in Section 5. Section 6 gives the experimental results. This study is concluded in Section 7.

2. Hydraulic Circuit

The hydraulic circuit of an EHA is shown in Fig. 1. A servo pump controls the flow of oil and a charge pump compresses oil in the hydraulic circuit. A relief valve is implemented to protect this hydraulic system. A servomotor drives the hydraulic pump only when it runs the hydraulic motor. This feature makes the EHA more energy efficient than previous open-loop hydraulic circuits. Furthermore, the actuator realizes backdrivability as the system is a closed circuit of the servo pump and the motor. Because the EHA circuit does not possess a servo valve, which would shut down the transmission of force when the valve is closed. Thus, the control performance is affected by resonance in the actuator. In general, EHAs have servo pumps as drives and hydraulic motors on the load-sides, which are expected to generate resonance via torsional twisting. Therefore, EHAs can be modeled as two-inertia systems in which two high-rigidity inertias are connected to each other via a low-rigidity shaft.

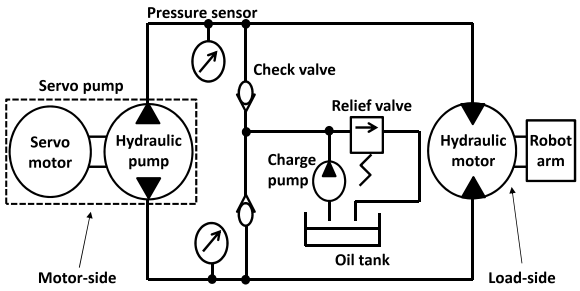

Fig. 1. Hydraulic circuit of EHA

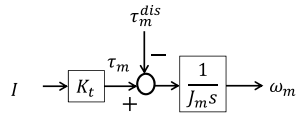

Fig. 2. Model of electric servo pump

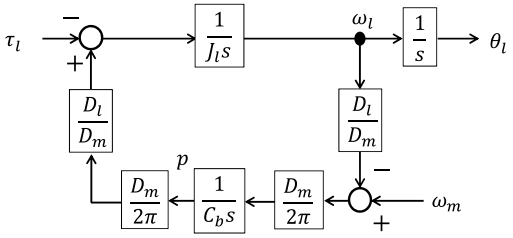

Fig. 3. Model of hydraulic actuator

2.1 Servo Pump In EHAs, the input current on the servomotor drives the pumps to generate torque. Figure 2 shows a block diagram from input current I to output angular velocity of the motor ω_m, where τ^{dis} represents the disturbance torque, K_t and J_m denote a torque constant and the inertia of the motor-side, respectively; m represents an index for the motor-side, l is an index for the load-side, and s expresses a Laplace operator. All the valuables in the figures are given as Laplace-transformed variables.

2.2 Hydraulic Actuator Referring to the model of Lee [9], a block diagram of a hydraulic actuator in which the angular velocity of the servomotor and the angle of the hydraulic motor are the input and output, respectively, can be expressed as shown in Fig. 3. Supposing that the leakage of hydraulic oil and viscous friction can be neglected, the motion equation of the hydraulic actuators can be given as (1), where D, p, C_b, and J are the displacement volume of the oil pump, pressure difference, a compressibility factor, and inertia of the motor, respectively. Here, q stands for the oil flow given by the model.

$$q(s) = \frac{D_m}{2\pi} s\theta_m(s) = \frac{D_l}{2\pi} s\theta_l(s) + C_b s p(s) \cdots\cdots\cdots (1)$$

In this study, we consider the servomotor and hydraulic pump as the motor-side of the actuator that drives the hydraulic motor with the robot arm, which is the load-side.

2.3 EHA A plant model of EHAs combining the servomotor plus pump and the hydraulic motor is given in Fig. 4. According to this figure, an EHA can be seen as a two-inertia system, as shown in Fig. 5 [4]. Here, the disturbance force applied to the servomotor τ_m^{dis} corresponds to the reaction force caused on the hydraulic actuator. This model indicates that EHAs can be modeled as two-inertia systems.

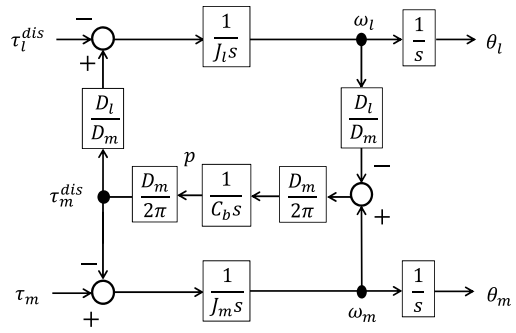

Fig. 4. Model of EHA

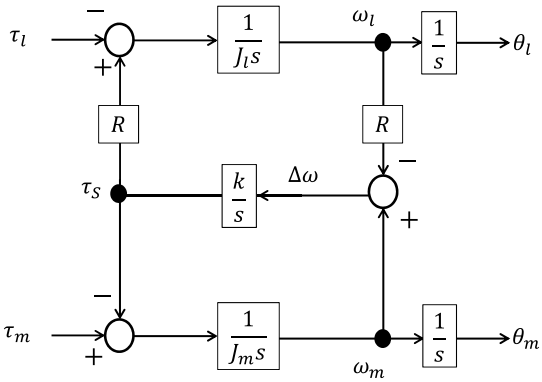

Fig. 5. Block diagram of two-inertia system

3. Two-inertia System

Figure 5 shows a general two-inertia system. As shown by the block diagram of Fig. 4, EHAs can be mathematically modeled as two-inertia systems, with each variable given by comparison of the plant models. According to Figs. 4 and 5, relationships between EHAs and two-inertia systems are given in (2) and (3). Here, the displacement-volume ratio of hydraulic motors and oil pumps corresponds to R and the compressibility of the oil is related to k.

$$R = \frac{D_l}{D_m} \quad \cdots\cdots (2)$$

$$k = \frac{1}{C_b}\left(\frac{D_m}{2\pi}\right)^2 \quad \cdots\cdots (3)$$

This model describes a servo pump with inertia J_m connected through a spring with torsional twist constant k to a load with inertia J_l. Here, θ, ω, τ, and R represent angle, angular velocity, torque, and reduction ratio, respectively. The relationships between torque input and motor's angle output are shown in (4) and (5).

$$\frac{\theta_{me}(s)}{\tau_m(s)} = \frac{1}{J_m s^2}\frac{s^2+\omega_z^2}{s^2+\omega_p^2} \quad \cdots\cdots (4)$$

$$\frac{\theta_l(s)}{\tau_m(s)} = \frac{1}{J_m s^2}\frac{\omega_z^2}{s^2+\omega_p^2} \quad \cdots\cdots (5)$$

Here, ω_p and ω_z are the resonance frequency and anti-resonance frequency, respectively. In this study, θ_m is a motor-side angle value and θ_{me} is a motor-side angle viewed from the load-side angle, which is given as $\theta_{me} = \theta_m/R$.

Equations (4) and (5) show that anti-resonance occurs only at the motor-side. Therefore, the phase of the load-side would have a delay of 180 degrees at frequencies equal to or higher than the resonance frequency; this issue would affect the bandwidth of feedback control. The resonance and anti-resonance frequencies can be determined from the experimental data. Thus, the inertial values of the motors are calculated by (6) and (7).

$$\omega_p = \sqrt{k\left(\frac{1}{J_m}+\frac{R^2}{J_l}\right)} \quad \cdots\cdots (6)$$

$$\omega_z = \sqrt{\frac{kR^2}{J_l}} \quad \cdots\cdots (7)$$

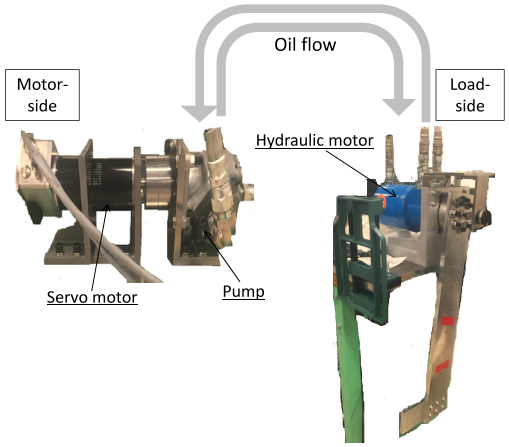

Fig. 6. EHA with one-link robotic arm

Fig. 7. Servo pump

4. Experimental Setup

Figure 6 shows the experimental setup used in this study; it consists of a hydraulic actuator with a robotic arm with one degree of freedom. The hydraulic motor was an orbit motor (Eaton). The rotation angle of the motors was measured by a 17-bit absolute encoder.

4.1 Servo Pump Figure 7 shows a servo pump that regulates the flow discharged into the motor. The input shaft of the hydraulic pump and the output shaft of the servomotor were coupled as the servo pump. The rotation angle of the servomotor was given by a 17-bit absolute encoder. The servomotor was a direct-drive DC blush-less E-60 motor (Maxon). The hydraulic pump was an MA-03 trochoid pump (Eaton).

4.2 Charge Pump Figure 8 shows the charge pump that oils and pressurizes the hydraulic circuit. The charge pressure was 5 MPa. The relief valve that regulated the pressure of the circuit and the oil tank, which held 3 l of oil, were coupled to the charge pump.

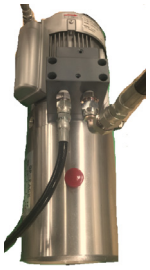

Fig. 8. Charge pump

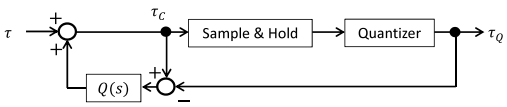

Fig. 9. Block diagram of feedback modulator

5. Controllers

5.1 Feedback Modulators The hydraulic actuators exhibit dead zones in the low-speed domain due to static friction. For that reason, the frequency characteristics of the experimental setup cannot be measured when the hydraulic motor drives in the low-speed domain. The input torque of the servomotor has to be larger than the maximum static-friction force of the hydraulic motor in order to drive the actuator at the dead zone. This problem is solved by quantizing the input torque. However, this method causes quantization errors. Thus, we apply the FMs, which can compensate for quantization errors that occur in the low-speed domain. FMs are dynamic quantizers with simple structures that do not require system models [32]. A block diagram of an FM is given in Fig. 9.

The FM is given by a low-pass filter $Q(s)$ satisfies $1 - Q(s) = (\frac{sT}{sT+1})^2$. The time constant T is given by $T = aT_S (a > 1)$, and a represents the time-constant ratio. Here, T_S represents sampling time. The relationships among the input torque τ, its quantized value τ_Q, and the quantization error $e = \tau_C - \tau_Q$ are given as (8). The input torque of the servomotor is given as $\tau_m = \tau_Q$.

$$\tau_m(s) = \tau_Q(s) = \tau(s) + (1 - Q(s))e(s) \cdots\cdots\cdots\cdots \quad (8)$$

In this study, the torque reference is quantized only while the angular velocity of the hydraulic motor is lower than the condition $\omega_{th} = 0.01$ rad/s, as has been studied [32]. The input-current value of the servomotor is given by quantized torque τ_Q, where K_t is the torque constant: $I = \frac{\tau_m}{K_t}$. Equation (9), which expresses the quantization of the input torque, is shown in the time domain as the variables are written with (t). Thus, these variables have the following relationships: $\tau_Q(s) = \mathcal{L}[\tau_Q(t)]$ and $\tau_C(s) = \mathcal{L}[\tau_C(t)]$.

$$\tau_Q(t) = \begin{cases} \tau_C(t) & (|\omega_l| > \omega_{th}) \\ \lfloor \tau_C(t)/d + 1 \rfloor d & (0 \le \omega_l \le \omega_{th}) \\ \lfloor \tau_C(t)/d - 1 \rfloor d & (-\omega_{th} \le \omega_l < 0) \end{cases} \cdots\cdots (9)$$

Here, $\lfloor\rfloor$ is a floor function, with d being a design parameter that is greater than the maximum static-friction force. These conditions suggest that the quantized torque is free from static friction in the low-speed domain.

5.2 Resonance Ratio Control The proposed controller used in this study is shown. Resonance-ratio control is a known vibration-suppression technique for two-inertia systems; it employs a feedback controller and disturbance observers (DOBs) designed by matching resonance frequencies to realize stable vibration-suppression control [15][25]. However, DOBs cause resonance in two-inertia systems because of the presence of a motor's inertia and torsional twisting between the motor and load. Resonance worsens the control performance in the system. Moreover, when the hydraulic motor is not rotating because of a large static-friction force, integrators over-accumulate response errors. Thus, it has been proposed that integrators such as DOBs should not be updated while the actuators stop in the dead zone, so as to avoid overcompensation of the friction force [32]. Based on the reported method to avoid updating DOBs, the proposed controller contains a memory to store the disturbance torque before updates. The conventional controllers also use the reported method to avoind updating the integrators for the comparison with the proposed controller.

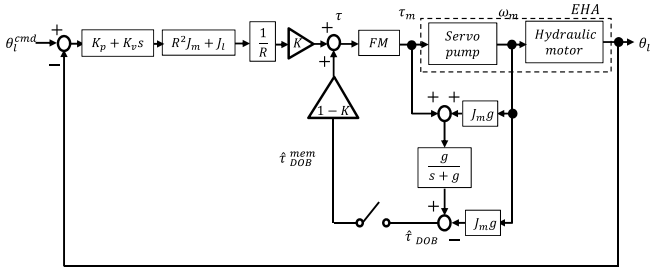

Fig. 10. Controller of resonance ratio control

A block diagram of the resonance ratio control is given in Fig. 10, in which the FM is shown as FM. While the DOB is not updated, $\hat{\tau}_{DOB}^{mem}$ holds the value of the DOB. The servomotor coupled with the pump is given as *Servo pump* and the hydraulic motor with the arm, which is the load-side, is given as *Hydraulic motor*.

6. Experiment

6.1 Parameter Identification Here, we verified the frequency characteristics from the input torque to the output angle of the hydraulic motor. We investigated whether or not the experimental setup showed the characteristics explained in (4) and (5) in order to prove the presence of the two-inertia resonance in the EHA. Figure 11 shows the frequency response from the torque reference to the load-side angle. This bode plot indicates that the EHA showed the same characteristics as the two-inertia resonance described in the Section 3. Here the resonance and anti-resonance frequencies were 7 Hz and 6.7 Hz, respectively. To the best of the authors' knowledge, this is the first study to investigate the resonance characteristics of EHAs.

The inertia of both the motor and load-sides were also calculated through this experiment. A weight was put on the robot arm to identify the inertia of the load-side of the EHA. Because of the change in the inertia of the load-side, both resonance and anti-resonance frequencies changed. Here, the inertia of weight ΔJ, which was given by the difference between J_l and J_l', and which corresponds the inertia of the weighted robot arm, was obtained by calculation.

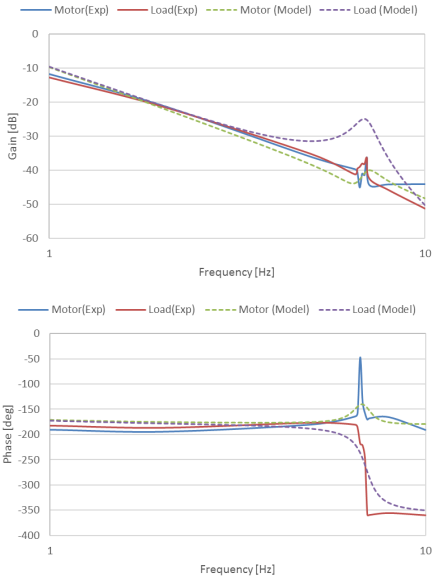

Fig. 11. Experimental frequency responses of EHA without weight

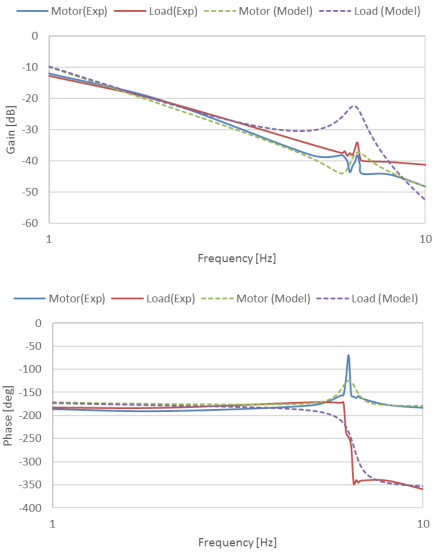

Fig. 12. Experimental frequency responses of EHA with weight

Equation (10) shows the relationship between the new anti-resonance frequency and the inertia.

$$\omega_z' = \sqrt{\frac{kR^2}{J_l'}} = \sqrt{\frac{kR^2}{J_l + \Delta J}} \cdots\cdots\cdots\cdots\cdots\cdots (10)$$

Since the torsional-twisting constant k did not change, k, J_m, and J_l were identified from the resonance characteristics of EHA with weight and without it using (6), (7), and (10). A bode plot of the EHA with the weight is shown in Fig. 12. Figure 13 shows a picture of the robot arm with the weight. The resonance and anti-resonance frequencies were 6.6 Hz and 6.3 Hz, respectively. Here, the experimental results are shown with simulated results based on the two-inertia system in Fig. 5. As a result, we not only found out the occurrence of the resonance on the EHA, but the inertia of both the motor-side and load-side of the experimental setup. Collected results are shown in Table 1. Moreover, this result

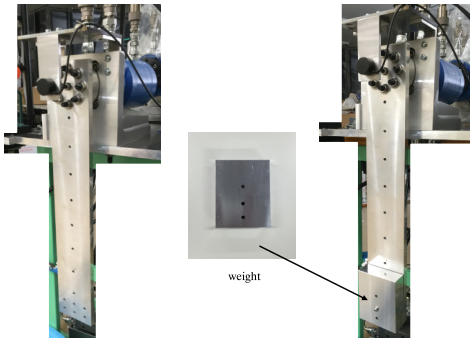

(a) Without weight (b) With weight

Fig. 13. Weight on robot arm

Table 1. Identified parameters

	Without weight	With weight
Resonance frequency [Hz]	7.00	6.60
Anti-resonance frequency [Hz]	6.70	6.30
Inertia of motor-side J_m[kgm^2]	0.000633	0.000564
Inertia of load-side J_l[kgm^2]	0.841	0.951
Inertia of weight on robot arm ΔJ[kgm^2]		0.110
Torsional twisting constant k[Nm/rad]	0.0915	0.0915

indicates that the experimental EHA could be considered as a two-inertia-resonance system. Thus, we can conclude that the established control methods for two-inertia systems are applicable to EHAs.

6.2 Performance of Position Response The proportional-derivative (PD)-control method was used to investigate the control performance of EHAs in the earlier study [11]. Sakaino investigated the performance of the PD control with the DOB along with the FM [32]. Therefore, the performance of the proposed method was evaluated by comparison with the proportional-integral-derivative (PID) control, as well as PD control with the DOB since it was mentioned as an extension of the earlier study [11]; these are general control methods for two-inertia systems. The integrators of conventional methods were not updated in the dead zone as well as the proposed method as this technique applied to the PD control with the DOB in the previous research [32]. The DOB was designed based on the experimentally determined parameters and resonance characteristics. For the design of the controller, the appropriate feedback gain of shaft twisting torque K was obtained by trial-and-error in this proposed controller. In the controller given in Fig. 10, the feedback of the DOB was multiplied by $(1 - K)$ and the inertia of the motor-side was multiplied by $1/K$ around the resonance frequency such that the vibration was suppressed.

Figure 14 shows the position responses of two conventional controllers compared to the proposed method. Here, broken and solid lines denote angle commands and responses of the hydraulic motor, respectively. The experimental parameters are shown in Table 2. Figure 15 shows the robustness of the proposed method considering modeling errors. Figure 16 gives the effect caused by K.

Figure 14(a) shows that PID-control caused phase delay because the integrator stopped updating with the use of the FM. In Fig. 14(b), the DOB could not suppress oscillation because of two-inertia resonance. Unlike the two conventional methods, the proposed controller suppressed oscillation in

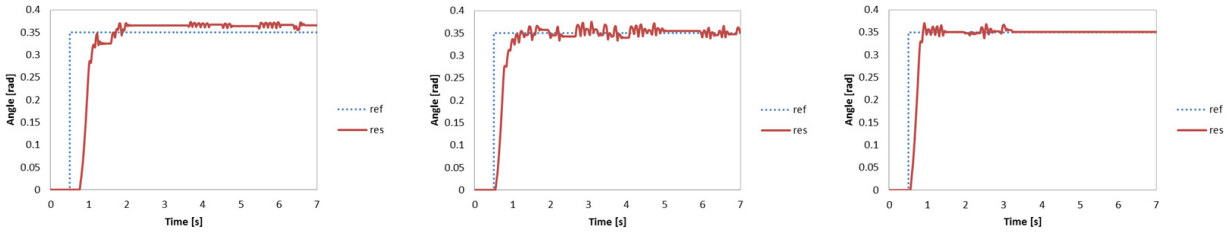

(a) PID (b) PD+DOB (c) Proposed method

Fig. 14. Step response

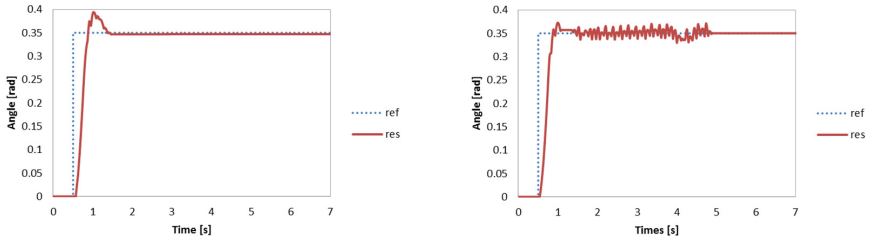

(a) $J_n = J/2$ (b) $J_n = 2J$

Fig. 15. Step response considering modeling error

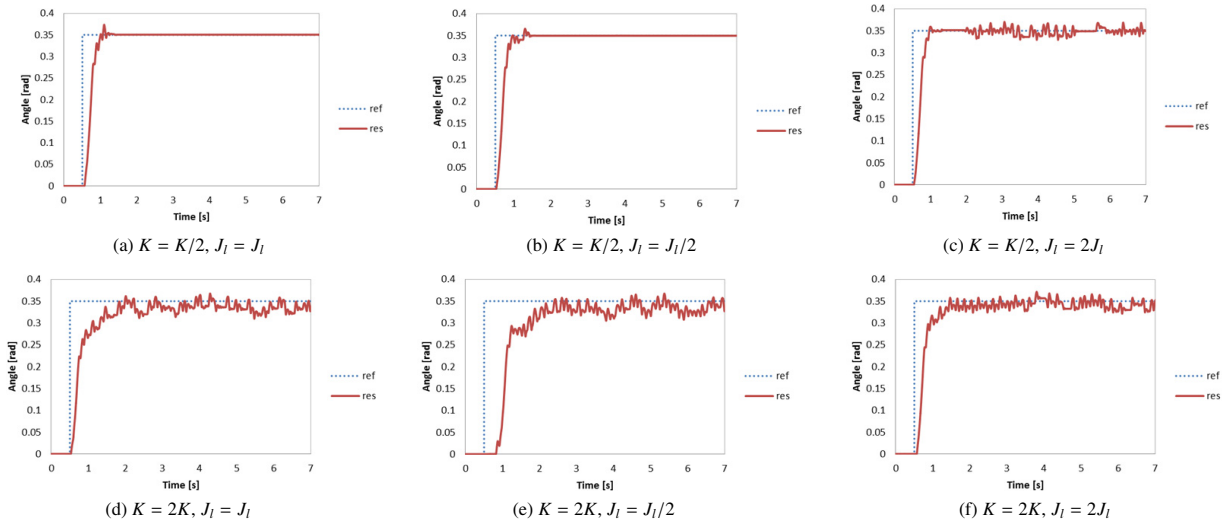

(a) $K = K/2$, $J_l = J_l$ (b) $K = K/2$, $J_l = J_l/2$ (c) $K = K/2$, $J_l = 2J_l$

(d) $K = 2K$, $J_l = J_l$ (e) $K = 2K$, $J_l = J_l/2$ (f) $K = 2K$, $J_l = 2J_l$

Fig. 16. Step response different considering K and modeling error

Fig. 14(c). Moreover, the proposed method's DOB compensated for steady-state errors thanks to the resonance-ratio technique. In short, the proposed method had the best control performance among these controllers.

In Fig. 15, the robustness of the proposed method was verified when the motor-side and load-side inertias had modeling errors. Here, J_n represents nominal inertia of motors given as $J_n = (J_{mn}, J_{ln})$, where J_{mn} and J_{ln} refer to the nominal inertias of the motor-side and load-side, respectively. J is given as $J = (J_m, J_l)$, representing both motor and load-side inertia identified in Table 1. This study considers only the control performance of the proposed method with the modeling error, since it was superior to the conventional methods, which did not suppress oscillation. Figure 15(a) shows tiny steady-state error, however, the proposed method suppressed the oscillation well. In Fig. 15(b), although more oscillation is shown in the response than in Fig. 15(a), the position response converged with the command finely. In short, the result shows that the proposed method maintained its control performance under modeling errors.

Figure 16 investigates the control performance with different K and modeling errors. When K is small, the effect of PD control becomes less dominant and the DOB has larger effect. Figure 16 illustrates that the proposed method maintains the robustness with model error. On the other hand, when K is large, the PD controller has a larger effect, causing oscillatory responses by the actuator. The proposed method did not possess the robustness of the control performance with large K.

The bandwidths of the proposed controller were 1.25 Hz on the motor-side and 1.31 Hz on the load-side.

7. Conclusion

This paper modeled EHAs as two-inertia systems and proposed a method to identify their dynamic characteristics. The frequency characteristics of an EHA with a one-link robotic arm were measured experimentally to determine if the EHA experienced sympathetic vibration. The results confirmed that resonance occurred, verifying that the two-inertia system could be applied for the identification of parameters. To

Table 2. Parameters

Nominal inertia of motor J_{mn}	kgm^2	
Nominal inertia of load J_{ln}	kgm^2	
Displacement of pump D_m	cm^3/rev	3.08
Displacement of motor D_l	cm^3/rev	393
Reduction ratio R		127.6
Resonance frequency ω_p	rad/s	43.9
Anti-resonance frequency ω_z	rad/s	42.1
Feedback gain of shaft twisting torque K		1.60
Proportional gain K_p	1/s^2	200
Integral gain K_i	1/s^3	30.0
Derivative gain K_d	1/s	20.0
Cut-off frequency of DOB g	rad/s	40.0
Time-constant ratio a		1.05
Sampling time T_S	s	0.001
Angle θ	rad	
Angular velocity ω	rad/s	
Current I	A	
Torque τ	Nm	
Force f	N	
Quantity of oil flow q	L/min	
Pressure of oil p	Pa	
Compressibility of oil C_b	m^5/N	
Time constant T	s	

decrease the static friction of the actuator, a FM was applied. To suppress the vibration in the EHA, resonance-ratio control was designed based on the experimentally determined parameters. The performance of the EHA was evaluated by comparison to the PID and PD control with the DOB in the position-response experiment. The results indicated that the proposed method, which introduced the resonance-ratio technique, was valid in terms of both the accuracy of control and suppression of the oscillation by the experiment. Besides the superior accuracy of the proposed method, the experimental results showed their robustness under modeling errors. This study did not consider oil leakage from the hydraulic motor. Thus, the results included uncertainties in the accuracy of the identified parameters. For this reason, it is necessary to implement further compensation for nonlinear elements to improve the accuracy of both the control systems and parameters. We will pursue this as future work.

References

(1) H. Kazerooni: Exoskeletons for human power augmentation, In Intelligent Robots and Systems, 2005. (IROS 2005). 2005 IEEE/RSJ International Conference on, pp.3459–3464, IEEE (2005)

(2) H. Kaminaga, J. Ono, Y. Nakashima, and Y. Nakamura: Development of backdrivable hydraulic joint mechanism for knee joint of humanoid robots, In Robotics and Automation, 2009. ICRA'09. IEEE International Conference on, pp.1577–1582, IEEE (2009)

(3) S. Sakaino, T. Furuya, and T. Tsuji: "Bilateral control between electric and hydraulic actuators using linearization of hydraulic actuators", *IEEE Trans. on Industrial Electronics* (2017)

(4) S. Sakaino and T. Tsuji: "Development of friction free controller for electro-hydrostatic actuator using feedback modulator and disturbance observer", *ROBOMECH Journal*, Vol.4, No.1, p.1 (2017)

(5) H. Kaminaga, H. Tanaka, and Y. Nakamura: "Mechanism and control of knee power augmenting device with backdrivable electro-hydrostatic actuator," In Proc. of 13th World Congress in Mechanism and Machine Science, No.A12, p.534 (2011)

(6) H. Kaminaga, T. Amari, Y. Katayama, J. Ono, Y. Shimoyama, and Y. Nakamura: "Backdrivability analysis of electro-hydrostatic actuator and series dissipative actuation model", In Robotics and Automation (ICRA), 2010 IEEE International Conference on, pp.4204–4211, IEEE (2010)

(7) H. Kaminaga, T. Amari, Y. Niwa, and Y. Nakamura: "Development of knee power assist using backdrivable electro-hydrostatic actuator", In Intelligent Robots and Systems (IROS), 2010 IEEE/RSJ International Conference on, pp.5517–5524 (2010)

(8) S.R. Habibi and R. Burton: "Parameter identification for a high-performance hydrostatic actuation system using the variable structure filter concept", *Journal of Dynamic Systems, Measurement, and Control*, Vol.129, No.2, pp.229–235 (2007)

(9) I. Lee, T. Kim, and S. Choi: "Hydraulic servo system using a feedback linearization controller and disturbance observer -sensitivity of system parameters", In Proceedings of the JFPS International Symposium on Fluid Power, Vol.2008, pp.307–312. Japan Fluid Power System Society (2008)

(10) R. Liu and A. Alleyne: "Nonlinear force/pressure tracking of an electro-hydraulic actuator", *Journal of dynamic systems, measurement, and control*, Vol.122, No.1, pp.232–236 (2000)

(11) W.Y. Lee, M.J. Kim, and W.K. Chung: "An approach to development of electro hydrostatic actuator (eha)-based robot joints", In Industrial Technology (ICIT), 2015 IEEE International Conference on, pp.99–106 (2015)

(12) L. An and N. Sepehri: "Hydraulic actuator leakage fault detection using extended kalman filter", *International Journal of Fluid Power*, Vol.6, No.1, pp.41–51 (2005)

(13) M.F. Rahmat, Z. Has, A.R. Husain, Y.M. Sam, K. Ishaque, R. Ghazaly, and S.M. Rozali: "Modeling and controller design of an industrial hydraulic actuator system in the presence of friction and internal leakage", *International Journal of the Physical Sciences*, Vol.6, No.14, pp.3502–3517 (2011)

(14) S. Tafazoli, P.D. Lawrence, S.E. Salcudean, D. Chan, S. Bachmann, and CW D. Silva: "Parameter estimation and actuator friction analysis for a mini excavator", In Robotics and Automation, 1996. Proceedings., 1996 IEEE International Conference on, Vol.1, pp.329–334, IEEE (1996)

(15) Y. Hori, H. Sawada, and Y. Chun: "Slow resonance ratio control for vibration suppression and disturbance rejection in torsional system", *Industrial Electronics, IEEE Transactions on*, Vol.46, No.1, pp.162–168 (1999)

(16) R. Oboe and D. Pilastro: "Use of load-side mems accelerometers in servo positioning of two-mass-spring systems", In Industrial Electronics Society, IECON 2015-41st Annual Conference of the IEEE, pp.004603–004608, IEEE (2015)

(17) C. Ma and Y. Hori: "Fractional order control and its application of pi/sup/spl alpha//d controller for robust two-inertia speed control", In Power Electronics and Motion Control Conference, 2004. IPEMC 2004. The 4th International, Vol.3, pp.1477–1482, IEEE (2004)

(18) S. Kukkonen and E. Mäkinen: "Performance of a pump controlled asymmetric actuator: A comparison of different control methods", In ASME/BATH 2014 Symposium on Fluid Power and Motion Control, pp.V001T01A001–V001T01A006. American Society of Mechanical Engineers (2014)

(19) H. Zeng and N. Sepehri: Tracking control of hydraulic actuators using a lugre friction model compensation, *Journal of Dynamic Systems, Measurement, and Control*, Vol.130, No.1, p.014502 (2008)

(20) C. Jing and H. Xu: "A study on the influence of friction on loading performance of electro-hydraulic friction load simulator for actuator test", In 2016 7th International Conference on Mechanical and Aerospace Engineering (ICMAE), pp.524–528 (2016)

(21) J. Yao, W. Deng, and Z. Jiao: "Adaptive control of hydraulic actuators with lugre model-based friction compensation", *IEEE Trans. on Industrial Electronics*, Vol.62, No.10, pp.6469–6477 (2015)

(22) A. Messina, N.I. Giannoccaro, and A. Gentile: "Experimenting and modelling the dynamics of pneumatic actuators controlled by the pulse width modulation (pwm) technique", *Mechatronics*, Vol.15, No.7, pp.859–881 (2005)

(23) T. Ohgi and Y. Yokokohji: "Control of hydraulic actuator systems using feedback modulator", *Journal of Robotics and Mechatronics*, Vol.20, No.5, p.695 (2008)

(24) S. Komada, M. Ishida, K. Ohnishi, and T. Hori: "Disturbance observer-based motion control of direct drive motors", *Energy Conversion, IEEE Transactions on*, Vol.6, No.3, pp.553–559 (1991)

(25) S. Zhao and Z. Gao: "An active disturbance rejection based approach to vibration suppression in two-inertia systems," *Asian Journal of Control*, Vol.15, No.2, pp.350–362 (2013)

(26) K. Szabat and T. Orlowska-Kowalska: "Vibration suppression in a two-mass drive system using pi speed controller and additional feedbacks-comparative study", *IEEE Trans. Industrial Electronics*, Vol.54, No.2, pp.1193–1206 (2007)

(27) J. Wang, Y. Zhang, L. Xu, Y. Jing, and S. Zhang: "Torsional vibration suppression of rolling mill with constrained model predictive control", In Intelligent Control and Automation, 2006. WCICA 2006. The Sixth World Congress on, Vol.2, pp.6401–6405. IEEE (2006)

(28) W. Li and Y. Hori: "Vibration suppression using single neuron-based pi fuzzy controller and fractional-order disturbance observer", *Industrial Electronics, IEEE Transactions on*, Vol.54, No.1, pp.117–126 (2007)

(29) S. Yamada, K. Inukai, H. Fujimoto, K. Omata, Y. Takeda, and S. Makinouchi: "Proposal of self resonance cancellation control without using drive-side information", In 41st Annual Conference of the IEEE Industrial Electronics

Society, pp.783–788, IEEE (2015)
(30) K. Yuki, T. Murakami, and K. Ohnishi: "Vibration control of 2 mass resonant system by resonance ratio control", In Industrial Electronics, Control, and Instrumentation, 1993. Proceedings of the IECON '93., International Conference on, pp.2009–2014 Vol.3 (1993)
(31) S. Sakaino and T. Tsuji: "Oil leakage and friction compensation for electro-hydrostatic actuator using drive-side and load-side encoders", In Industrial Electronics Society, IECON 2016-42nd Annual Conference of the IEEE, pp.5088–5093, IEEE (2016)
(32) S. Sakaino and T. Tsuji: "Integration of disturbance observer and feedback modulator for dead zone compensation of hydraulic actuator", In Industrial Electronics Society, IECON 2014-40th Annual Conference of the IEEE, pp.2786–2791, IEEE (2014)

Kenta Tsuda (Non-member) received the B.E. degree in the electrical and electronic systems from Saitama University, Saitama, Japan, in 2016. He is currently working on M.E. degree at the Department of Electrical and Electronic Systems from Saitama University. His research interests include motion control and mechatronics.

Tomoki Sakuma (Non-member) received the B.E. and M.E. degrees in the electrical and electronic systems from Saitama University, Saitama, Japan, in 2015, and 2017, respectively. He currently works at KAWASAKI HEAVY INDUSTRIES.

Kodai Umeda (Non-member) received the B.E. degree in the electrical and electronic systems from Saitama University, Saitama, Japan, in 2016. He is currently working on M.E. degree at the Department of Electrical and Electronic Systems from Saitama University. His research interests include motion control and mechatronics.

Sho Sakaino (Senior Member) received the B.E. degree in system design engineering and the M.E. and Ph.D. degrees in integrated design engineering from Keio University, Yokohama, Japan, in 2006, 2008, and 2011, respectively. He is currently an assistant professor with the Department of Electrical and Electronic Systems, Saitama University, Saitama, Japan. His research interests include mechatronics, motion control, robotics, and haptics. He received the IEEJ Industry Application Society Distinguished Transaction Paper Award in 2011.

Toshiaki Tsuji (Senior Member) received the B.E. degree in system design engineering and the M.E. and Ph.D. degrees in integrated design engineering from Keio University, Yokohama, Japan, in 2001, 2003, and 2006, respectively. He was a research associate in Department of Mechanical Engineering, Tokyo University of Science from 2006 to 2007. He is currently an associate professor with the Department of Electrical and Electronic Systems, Saitama University, Saitama, Japan. His research interests include mechatronics, motion control, haptics, and rehabilitation robots. He received the FANUCFA and Robot Foundation Original Paper Award in 2007 and 2008.